

Fermi National Accelerator Laboratory

FERMILAB-Pub-78/52-EXP
7180.288

(Submitted to Phys. Rev. Lett.)

STUDY OF SCALING IN HADRONIC PRODUCTION OF DIMUONS

J. K. Yoh, S. W. Herb, D. C. Hom, L. M. Lederman,
J. C. Sens, and H. D. Snyder
Columbia University, New York, New York 10027

and

K. Ueno, B. C. Brown, C. N. Brown, W. R. Innes,
R. D. Kephart, and T. Yamanouchi
Fermi National Accelerator Laboratory, Batavia, Illinois 60540

and

R. J. Fisk, A. S. Ito, H. Jöstlein, and D. M. Kaplan
State University of New York, Stony Brook, New York 11974

June 1978



STUDY OF SCALING IN HADRONIC PRODUCTION OF DIMUONS

J. K. Yoh, S. W. Herb,^{a)} D. C. Hom, L. M. Lederman,
J. C. Sens, and H. D. Snyder
Columbia University
New York, New York 10027

and

K. Ueno, B. C. Brown, C. N. Brown, W. R. Innes,
R. D. Kephart, and T. Yamanouchi
Fermi National Accelerator Laboratory
Batavia, Illinois 60510

and

R. J. Fisk, A. S. Ito, H. Jöstlein, and D. M. Kaplan
State University of New York
Stony Brook, New York 11974

ABSTRACT

We present proton-nucleus dimuon production cross sections for masses between 4 and 15 GeV, center of mass rapidities between -0.3 and 0.7 and incident energies of 200, 300, and 400 GeV. The data confirm scaling to the 20% level. The dependence of continuum $\langle p_T \rangle$ on beam energy is also presented.

^{a)} Present address: Foundation for Fundamental Research on Matter, the Netherlands.

We have extended our study of muon pair production by 400 GeV protons¹ to incident proton energies of 200 and 300 GeV. We find that a dimensionless form of the cross section can be well described at all three beam energies by a single function that depends only on dimensionless variables. Scaling of the cross sections in this manner implies the absence of any mass parameters with values similar to the relevant variables in the process, in this case the mass of the muon pair ($4 \leq m \leq 15$ GeV) and the total CM energy \sqrt{s} . An extensive literature² has appeared in which issues of scale breaking, asymptotic freedom and QCD act to modify the qualitatively successful parton annihilation model. It is these issues that we hope will be illuminated by the data presented here.

Figure 1 shows our mass spectra evaluated for the mean CM rapidity y of each data sample. We have fit these data excluding the 8.8-11 GeV (T) region with linear exponential curves, subtracted the fit from the data, and tested the remainder for enhancements in the excluded region. We list the results of the continuum and the T fits³ in Table I. We note that the acceptance in y is roughly Gaussian with a full width of 0.4 units. Since the laboratory angle of the spectrometer is fixed, the center of this acceptance shifts with incident beam energy as indicated in Table I.

In Fig. 2 we present a dimensionless form of the cross section, $s \frac{d^2\sigma}{d\sqrt{\tau} dy}$ in bins of $\sqrt{\tau} = M/\sqrt{s}$ as a function of y . We assume a dimuon decay distribution $1 + \cos^2\theta$ in the Gottfried-Jackson frame and integrate over dimuon transverse momentum p_T ;

data in the T region have been excluded. The major systematic uncertainty is the relative normalization between data taken at different beam energies. We estimate $\pm 5\%$ between 200 and 300 GeV and $\pm 10\%$ between 200/300 and 400 GeV. We note that the acceptance in y is far from ideal for purposes of extracting y behavior. This results in an extra systematic uncertainty of $\pm 10\%$ at the acceptance edges. If scaling is assumed, the data in Fig. 2 represent measurements of the y dependence for $-0.3 < y < .7$.

In Fig. 3(a), we present the cross sections at $y = .2$ (where all three energies overlap) vs. $\sqrt{\tau}$. We find the results consistent with a global fit:⁴

$$s \frac{d^2\sigma}{d\sqrt{\tau} dy} \Big|_{y=.2} = (44. \pm 0.7 \pm 12.0) \mu\text{b GeV}^2 e^{-(25.3 \pm .2 \pm .6)\sqrt{\tau}} \quad (1)$$
$$\chi^2/DF = 173/145 \text{ (confidence level} = 10\%).$$

Figure 3(b) displays the ratio of the cross section of Fig. 3(a) and this global fit. The contrast between figures 1 and 3 illustrates the significance of the scaling test. We note that scale breaking at the level observed in deep inelastic scattering would have no effect at $\sqrt{\tau} = 0.2$ and would cause the 200 GeV data points to be on the order of $\sim 20\%$ above the 400 GeV data at $\sqrt{\tau} = 0.5$.

Figure 4 graphs the relative y slope of $s \frac{d^2\sigma}{d\sqrt{\tau} dy}$ at $y = 0$ vs. $\sqrt{\tau}$ for the 400 GeV data. Positive slopes indicate a strong forward backward asymmetry. One expects asymmetry since

our target nucleon is on average 40% proton and 60% neutron. Figure 4 also indicates that the observed y -behavior is consistent with that expected from the parton annihilation model fit to our 400 GeV data¹ with an SU_3 symmetric sea.

The naive parton annihilation model predicts that the p_T dependence of the invariant cross section should vary only with \sqrt{T} and y . We find the p_T dependence well represented by the form:

$$E \frac{d^3\sigma}{dp^3} = C(1 + (p_T/P_0)^2)^{-6} \quad (2)$$

with parameters P_0 and C given in Table II. Our results for $\langle p_T \rangle$ (calculated from the data) are shown in Fig. 5 along with data at lower masses.⁵ We have ascertained that $\langle p_T \rangle$ does not vary significantly over our y range.⁶ For $m > 5$ GeV, and excluding the T region, $\langle p_T \rangle$ is independent of mass but rises with beam energy. This may be described by:

$$\langle p_T^2 \rangle = \alpha + \beta s \quad m > 5 \text{ GeV} \quad (3)$$

where $\alpha = .70 \text{ GeV}^2$ and $\beta = .0018$. Although the disagreement with the naive parton annihilation model is clear, this result is not in contradiction with QCD calculations.² The parameter α presumably represents the "intrinsic" quark transverse momenta.

In conclusion, we have presented excitation data for T , T' and T'' production. The dimuon continuum cross sections scale over the energy and mass range studied. The y distributions

exhibit a forward peaking consistent with parton-annihilation models. The p_T distributions imply $\langle p_T \rangle$ increases with energy at fixed m/\sqrt{s} .

We wish to thank many people from the staffs of Fermilab, Nevis Labs, and S.U.N.Y., Stony Brook. This work was supported in part by the National Science Foundation and the U.S. Department of Energy.

REFERENCES

- ¹S. W. Herb et al., Phys. Rev. Lett. 39, 252 (77).
 W. R. Innes et al., Phys. Rev. Lett. 39, 1240 (77).
 D. M. Kaplan et al., Phys. Rev. Lett. 40, 435 (78).
²G. Altarelli et al., TH 2450-CERN, 1977.
 H. Fritzsche and P. Minkowski, TH. 2400-CERN, 1977.
 F. Halzen and D. M. Scott, University of Wisconsin Preprint, C000-811-21 (1978).
 Kajantie and R. Raitio Helsinki Preprint HU-TFI-77-21 (1977).
 J. Kogut Phys. Lett. 65B, 377 (1976).
 H. D. Politzer, Nucl. Phys. B129, 301 (1977).
 A. V. Radyushkin, Phys. Lett. 69B 245 (1977).

³The cross sections in Table I have been corrected for Fermi motion in the nuclear targets to yield the cross section at the \sqrt{s} for a proton-nucleon collision. This correction is approximately given by

$$d^2\sigma/dm dy \Big|_{\sqrt{s}} \text{ proton-nucleon collision}$$

= $e^{-.82(\sqrt{\tau} - .2)}$ $d^2\sigma/dm dy \Big|_{\sqrt{s}}$ observed for $.2 < \sqrt{\tau} < .5$. All other data reported here have not been corrected for Fermi motion.

⁴The relative normalizations between cross sections measured at different energies were treated as data with errors equal to their systematic uncertainties. The fit was:

	<u>Input</u>	<u>Fit</u>
400 GeV/300 GeV	1.0 ± .10	1.01 ± .01
200 GeV/300 GeV	1.0 ± .05	1.01 ± .03

⁵J. G. Branson et al., Phys. Rev. Lett. 38, 1334 (1977).

⁶We have examined separately the data with $P_T > 1$ GeV/c and observe no qualitative differences in the s or y behavior of this subset. The p_T dependence of dilepton production poses a serious challenge to perturbative QCD calculations. See Ref. 2.

TABLE I
Mass Fit Parameters (a), (b), (c)

P_{beam}	200	300	400
$\langle y_{\text{acceptance}} \rangle$	0.40	0.21	0.03
A nb/GeV	$10.4 \pm .11 \pm 2.2$	$2.47 \pm 0.03 \pm 0.5$	$2.70 \pm .02 \pm 0.5$
b GeV^{-1}	$1.39 \pm .02 \pm 0.02$	$1.04 \pm 0.01 \pm 0.02$	$0.97 \pm 0.01 \pm 0.02$
χ^2/DF	42/34	35/54	78/74
$m(\pi)$ GeV	9.46 (fixed)	$9.45 \pm 0.02 \pm 0.10$	$9.46 \pm 0.012 \pm 0.10$
B $d\sigma/dy$ pb	0.002 ± 0.002	0.094 ± 0.012	0.29 ± 0.012
$m(\pi' - \pi)$ GeV	0.6 (fixed)	$0.69 \pm 0.05 \pm 0.05$	$0.60 \pm 0.03 \pm 0.05$
B $d\sigma/dy$ π'/π	0.67 ± 0.94	$0.46 \pm 0.09 \pm 0.10$	$0.38 \pm 0.04 \pm 0.10$
$m(\pi'' - \pi)$	1.0 (fixed)	1.0 (fixed)	0.97 ± 0.10
B $d\sigma/dy$ π''/π	0.10 ± 0.55	0.00 ± 0.06	$0.08 \pm 0.04 \pm 0.04$
χ^2/DF	12.6/19	12.1/16	14.7/16
$T/\text{cont.}$ GeV	$0.1 \pm .1$	0.67 ± 0.10	0.97 ± 0.05
$T'/\text{cont.}$ GeV	-	0.58 ± 0.14	0.66 ± 0.08
$T''/\text{cont.}$ GeV	-	0.00 ± 0.13	0.19 ± 0.12

(a) Continuum form: $d\sigma/dm dy = A e^{-bm}$. Cross sections are evaluated at $y = \langle y \rangle_{\text{acceptance}}$.

(b) The first error is statistical and the second is systematic.

(c) See Ref. 3.

TABLE II
 P_T FIT PARAMETERS (a), (b)

\sqrt{s} (GeV)	19.4		23.7		27.3	
M	C (fb.GeV ⁻²)	P_o (GeV)	C	P_o	C	P_o
4.5	7169±208	2.07±.049	9006±250	2.25±.055	10310±419	2.62±.095
5.5	1592± 59	2.34±.055	2648± 79	2.41±.044	2887± 55	2.70±.035
6.5	470± 21	2.34±.061	842± 30	2.60±.055	1058± 25	2.74±.036
7.5	121±9.9	2.19±.099	326± 16	2.59±.068	386± 13	2.86±.050
8.5	26.3 ±4.4	2.01±.186	104±8.0	2.53±.097	163±6.4	2.78±.058
9.5	7.22±2.07	2.29±.393	70.5±5.5	2.65±.111	130±5.6	3.10±.075
10.5			19.3±3.0	2.65±.247	41.8±3.1	2.83±.112
11.5					10.2±1.9	2.21±.202

(a) $E \cdot \frac{d^3\sigma}{dp^3} = C(1 + (\frac{P_t}{P_o})^2)^{-6}$

(b) Significant data extend to about 3 GeV/c in p_T . See Kaplan et al. (Ref. 1).

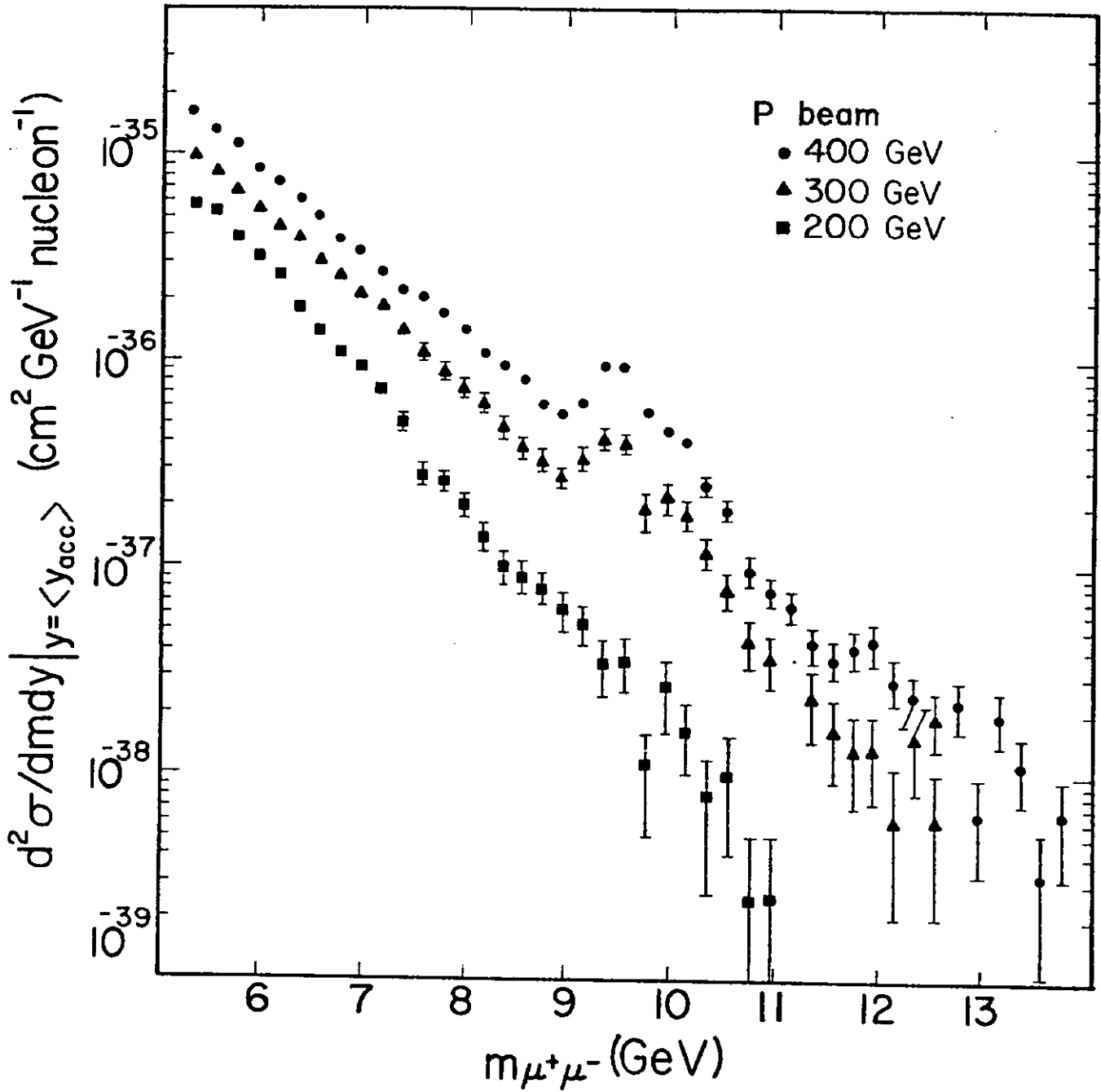


Fig. 1. $\frac{d^2 \sigma}{d m d y} \Big|_{y = \langle y_{acc} \rangle}$ vs. m for three beam energies.

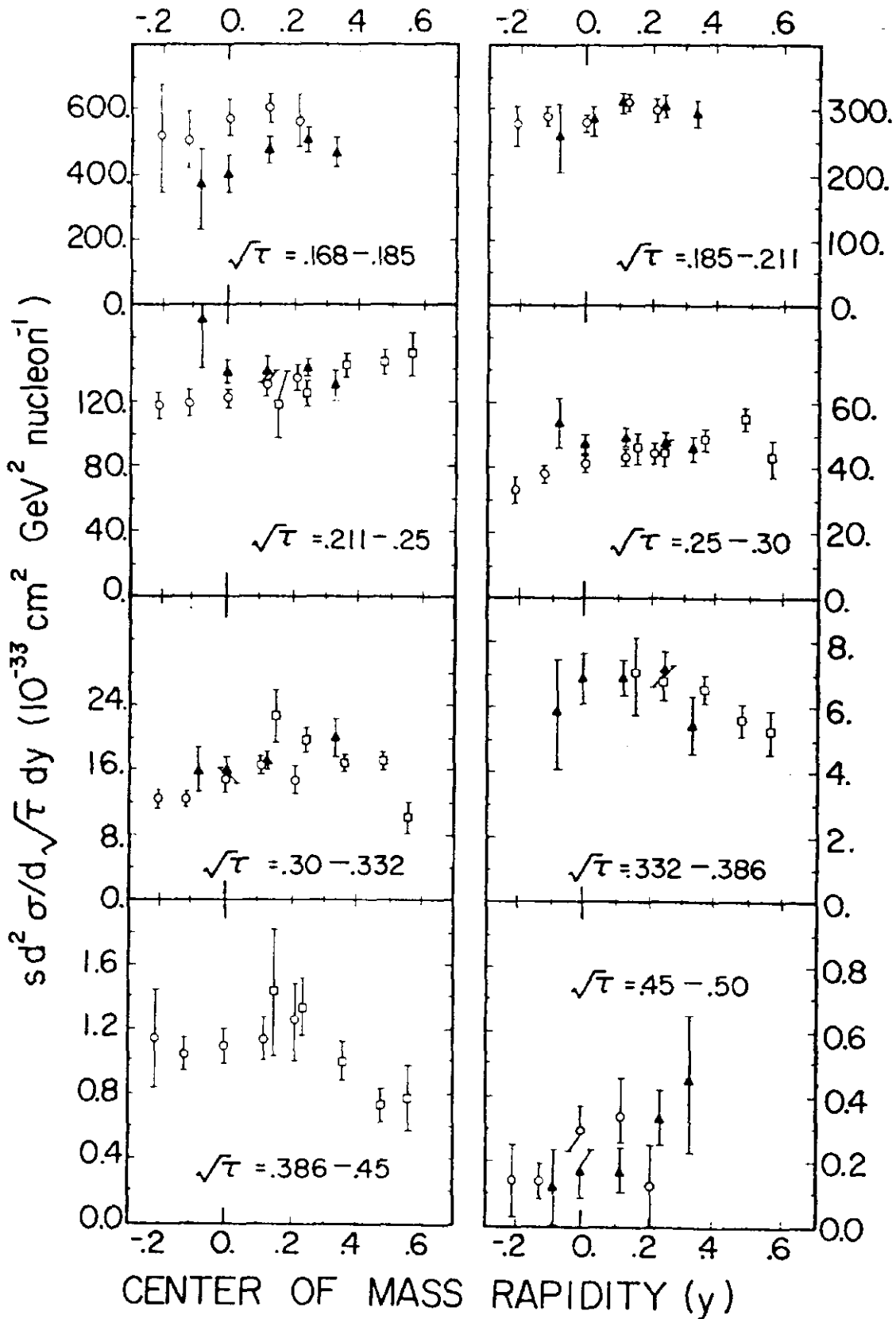


Fig. 2. $sd^2 \sigma/d\sqrt{\tau} dy$ vs. y for several $\sqrt{\tau}$ bins. Circles are $P_{\text{beam}} = 400$ GeV, triangles are 300 GeV, and squares are 200 GeV.

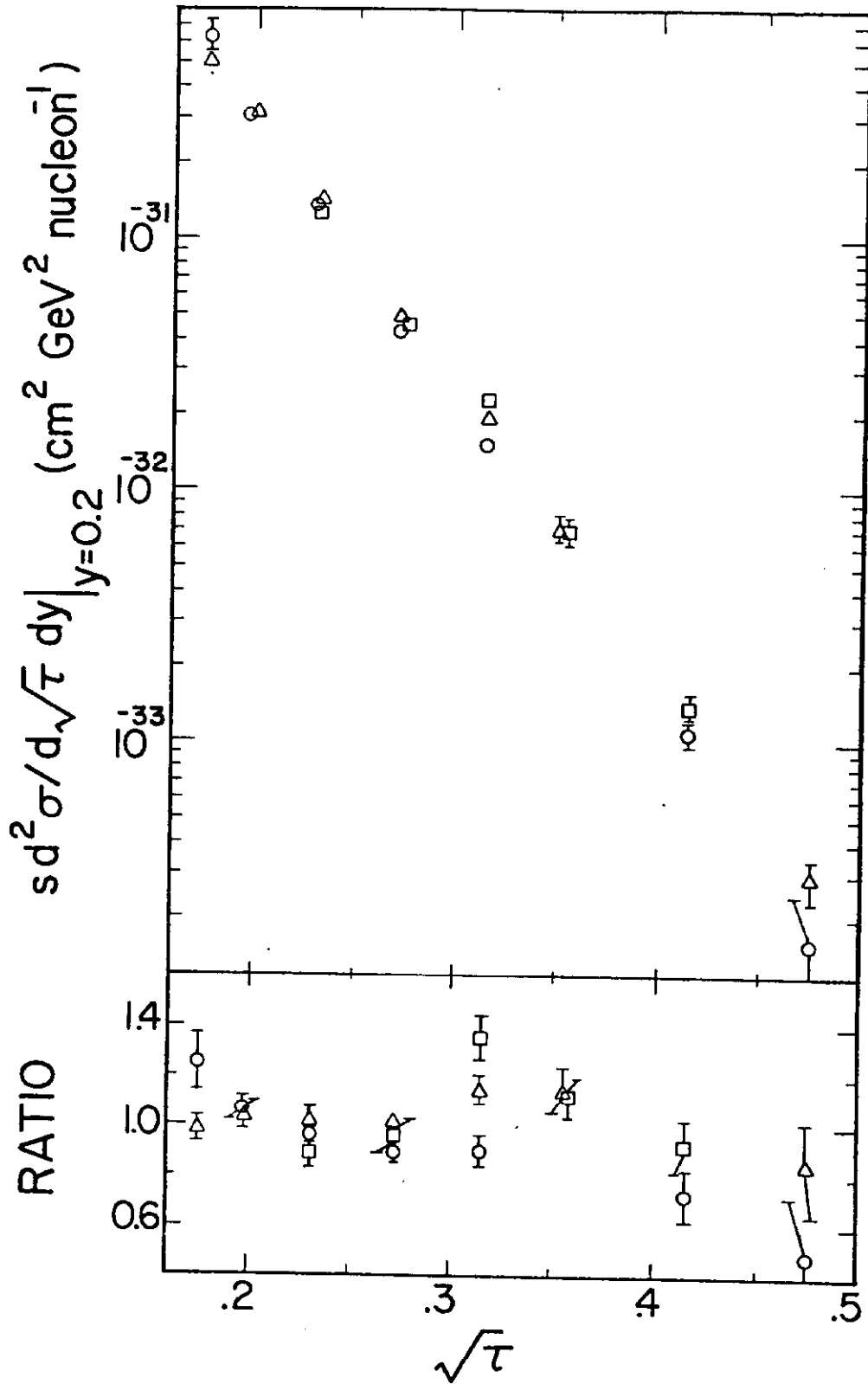


Fig. 3. (a) $sd^2\sigma/d\sqrt{\tau} dy|_{y=0.2}$ vs. $\sqrt{\tau}$. (b) Above data divided by the overall fit: $A e^{-b\sqrt{\tau}}$.

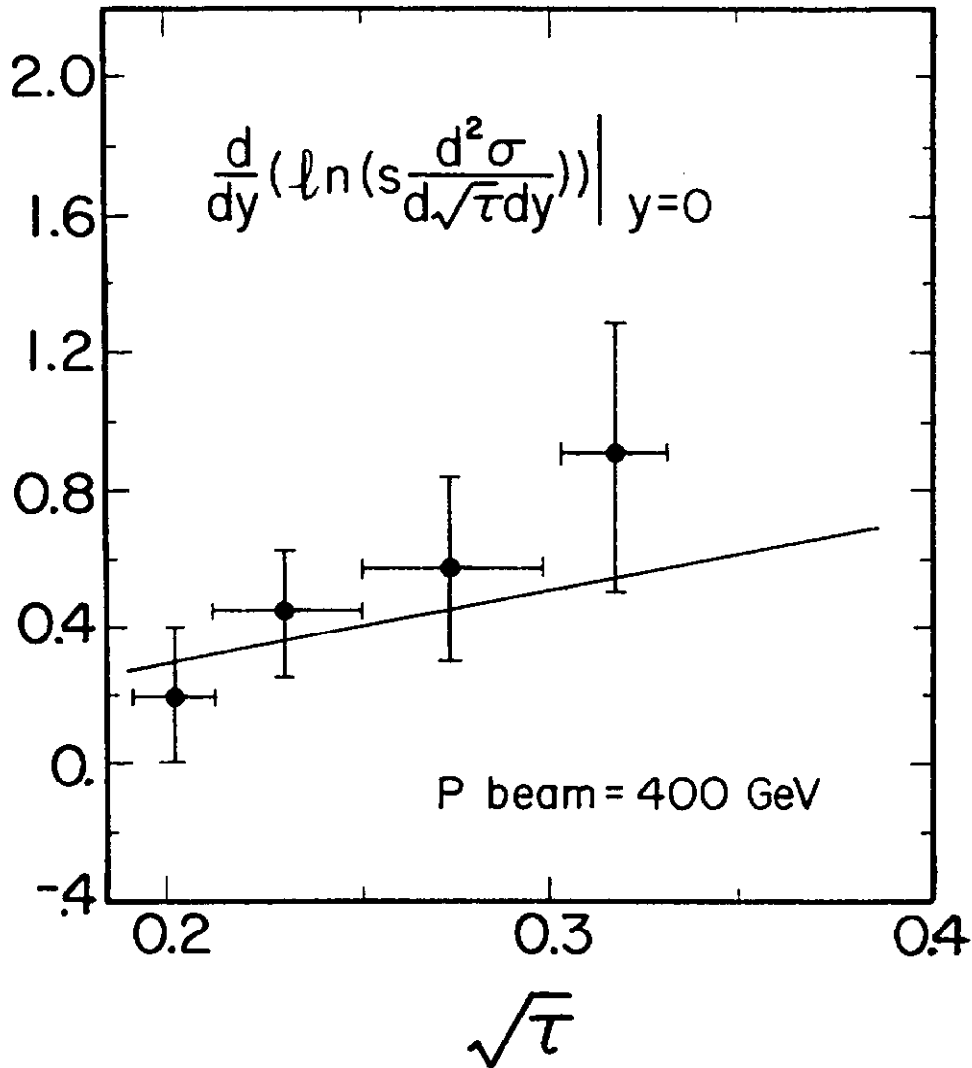


Fig. 4. The relative slope of the y distribution at $y = 0$ vs. $\sqrt{\tau}$ for the 400-GeV data. The curve is a result from a parton annihilation model calculation.

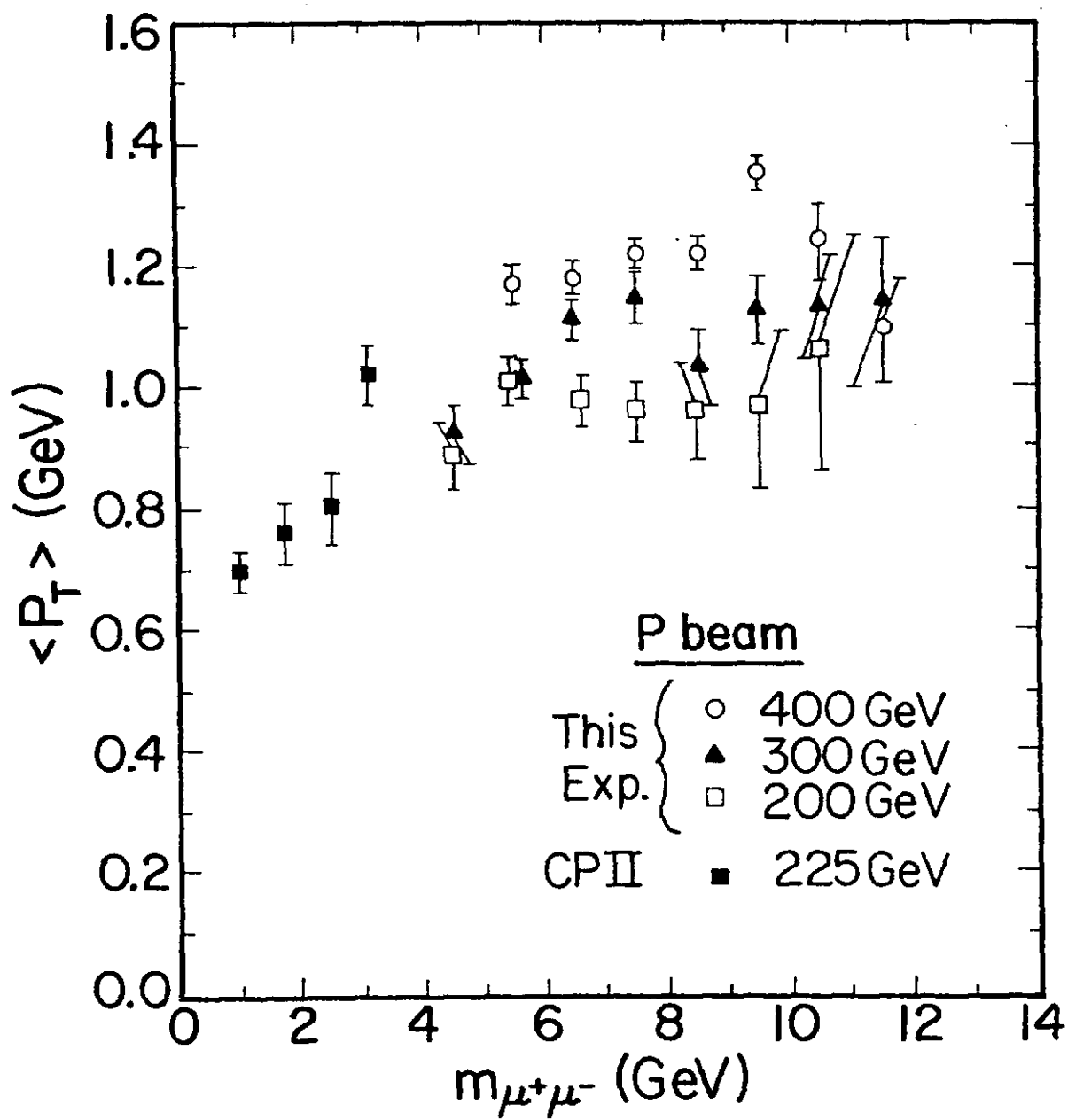


Fig. 5. $\langle P_T \rangle$ vs. m for three beam energies. The data below 4 GeV are from Ref. 5.